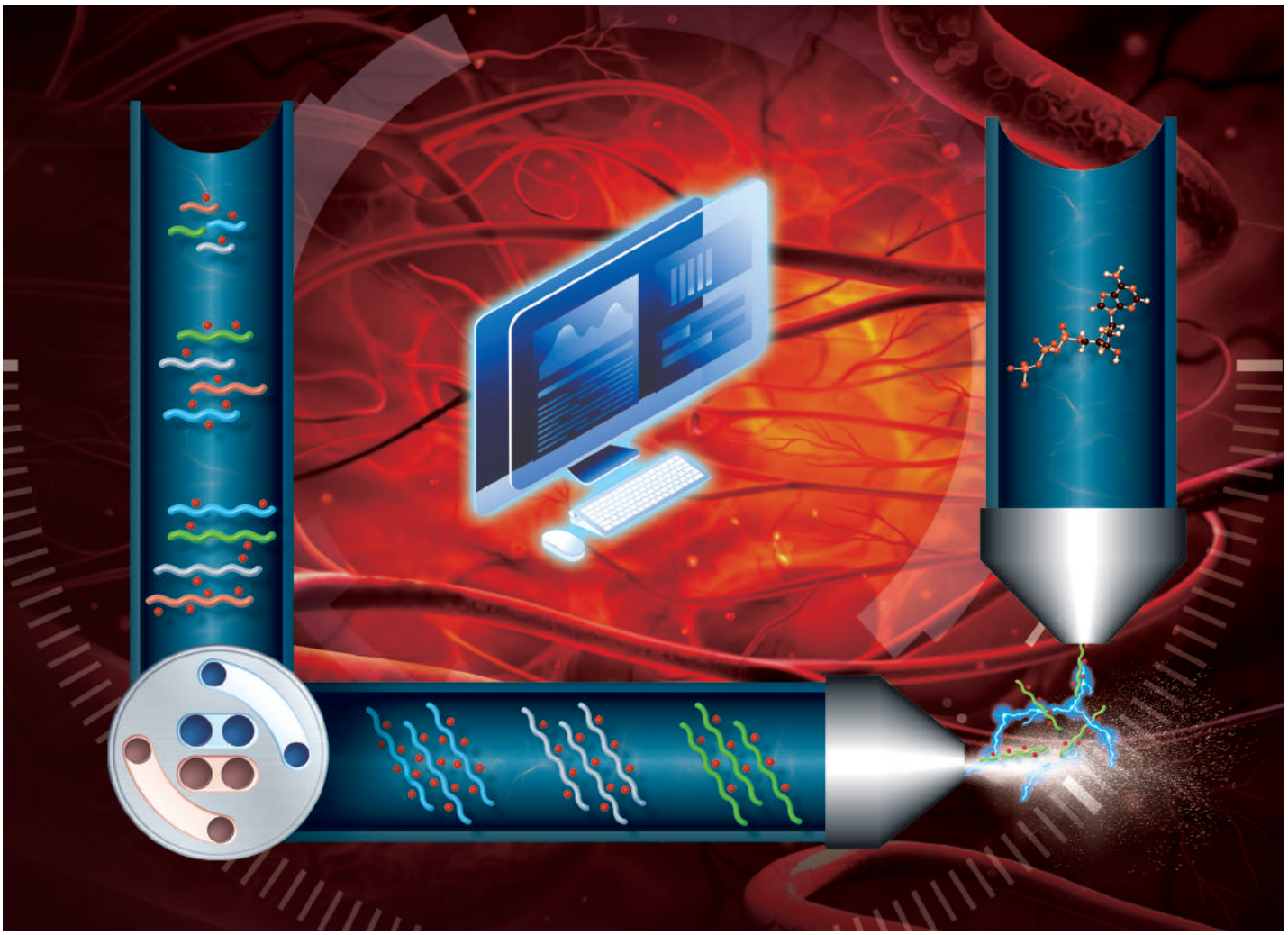

Showcasing research from Professor Zhenqing Zhang's laboratory, School of Pharmaceutical Sciences, University of Soochow University, Suzhou, China.

Systematic analysis of enoxaparins from different sources with online one- and two-dimensional chromatography

Enoxaparin, one of the most important low molecular weight heparins (LMWHs) is widely used as an anticoagulant. Enoxaparin is a product degraded from heparin. It has a molecular weight distribution and complex structural properties. The oligosaccharide size dispersity, structural compositions and fingerprinting profiles of 38 batches of enoxaparin were investigated in this work with multiple dimensional analysis approaches. The results showed its glycan size distribution is more related to the production process. Its disaccharide composition, sequence and the variety of glycans are more related to the AT binding-based anticoagulant activity.

As featured in:

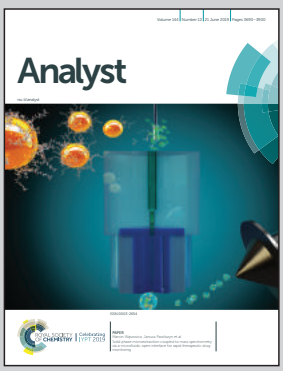

See Robert J. Linhardt, Zhenqing Zhang *et al.*, *Analyst*, 2019, **144**, 3746.

ROYAL SOCIETY OF CHEMISTRY | Celebrating IYPT 2019

rsc.li/analyst

Registered charity number: 207890

Analyst

PAPER

Cite this: *Analyst*, 2019, **144**, 3746

Systematic analysis of enoxaparins from different sources with online one- and two-dimensional chromatography†

Yilan Ouyang,[a,b] Meng Zhu,[a] Xin Wang,[c] Lin Yi,[a] Jawed Fareed,[d] Robert J. Linhardt *[b] and Zhenqing Zhang *[a]

Received 1st March 2019,
Accepted 3rd April 2019

DOI: 10.1039/c9an00399a

rsc.li/analyst

Enoxaparin, one of the most important low-molecular-weight heparins (LMWHs), is widely used as a clinical anticoagulant. Different production processes and animal sources of its precursor (unfractionated heparin) can result in the structural diversity of enoxaparin. In this study, 38 lots of enoxaparin prepared at different times, from different providers and animal sources, were systematically analyzed. SEC and SAX were used to analyze the oligosaccharide dispersity and structural compositions (disaccharide domains) of enoxaparins by size and charge, respectively. The results provide clues as to whether the structural variations in enoxaparin, observed in oligosaccharide mapping and/or disaccharide analysis, are attributable to differences in the animal sources of its heparin precursor or enoxaparin production processes based on times or brands. The representative enoxaparins were fingerprinted with online multiple heart-cut two-dimensional liquid chromatography-mass spectrometry (MHC-2DLC-MS). The profiles in MHC-2DLC-MS showed the detailed structural information of enoxaparins. In addition, the binding capacities to antithrombin III (AT) of these 38 lots of enoxaparins were detected using surface plasmon resonance (SPR) with the competitive inhibition mode. The results showed that the glycan size distribution of an enoxaparin is more related to its production process. The disaccharide composition, sequence and the variety of glycans of an enoxaparin are more related to its AT binding-based anticoagulant activity.

Introduction

Enoxaparin, developed in the 1980s, is one of the most important low-molecular-weight heparins (LMWHs) and is widely used as a clinical anticoagulant.[1,2] Enoxaparin is derived from heparin by benzylation and alkaline degradation.[3,4] Heparin, a linear and highly sulfated polysaccharide, has a polydisperse molecular weight (MW) and a complex structural composition.[5] It was discovered in dog liver in 1916.[6] Now, the most pharmaceutical heparin products are extracted from porcine intestinal mucosa. The weight average MW of heparin has been reported to be 15–18 kDa.[7] The sugar chains are structurally composed of the major repeating disaccharide unit, 2-*O*-sulfo-α-L-iduronic acid (IdoA2S) 1 → 4 linked to 6-*O*-sulfo, *N*-sulfo-α-D-glucosamine (GlcNS6S), as well as variable disaccharide units comprised of a β-D-glucuronic acid (GlcA), α-L-iduronic acid (IdoA) or IdoA2S 1 → 4 residue linked to 6-*O*-sulfo and/or 3-*O*-sulfo and/or *N*-sulfo (GlcNS) or *N*-acetylated (GlcNAc) α-D-glucosamine residues.[8,9] A rare pentasaccharide sequence comprises the antithrombin III (AT)-binding site, including GlcNAc/NS6S (1 → 4) GlcA (1 → 4) GlcNS3S and 6S (1 → 4) IdoA2S (1 → 4) GlcNS6S, which are important for heparin's anticoagulant activity (Fig. 1A).[10,11] The weight average MW of enoxaparin has been reported as 4.3–4.8 kDa.[12] Some of the relatively shorter glycan chains in enoxaparin retain their anticoagulant domain, corresponding to their AT-binding site, but these chains are too short to form heparin-AT-thrombin ternary complexes, which had been associated with heparin's bleeding side effects.[13] However, the reduced MW of enoxaparin does not decrease its structural complexity and like heparin it is a complex polycomponent drug. The

[a]*Jiangsu Key Laboratory of Translational Research and Therapy for Neuro-Psycho-Diseases and College of Pharmaceutical Sciences, Soochow University, Suzhou, Jiangsu 215021, China. E-mail: z_zhang@suda.edu.cn; Fax: +86-512-65882593; Tel: +86-512-65882593*

[b]*Center for Biotechnology and Interdisciplinary Studies, Rensselaer Polytechnic Institute, 110 8th Street, Troy, NY 12180, USA. E-mail: linhar@rpi.edu; Fax: +(518) 276-3405; Tel: +(518) 276-3404*

[c]*The Respiratory Department, Jinan Central Hospital Affiliated to Shandong University, Jinan, Shandong 250013, China*

[d]*Hemostasis and Thrombosis, Department of Pathology, Loyola University Medical Center, Maywood, IL, 60141, USA*

†Electronic supplementary information (ESI) available. See DOI: 10.1039/c9an00399a

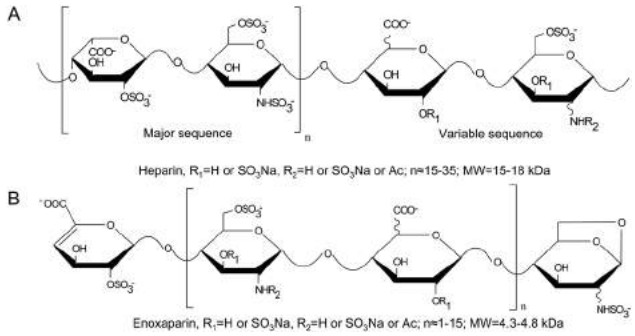

Fig. 1 The structures of heparin and enoxaparin.

alkaline degradation occurring at IdoA2S residues along heparin sugar chains forms additional structural moieties at both terminals on newly generated sugar chains. The unsaturated uronic acid and 1,6 anhydro glucosamine residues can occur at non-reducing and reducing terminals of enoxaparin glycans, respectively (Fig. 1B).[4] The structure of enoxaparin can also be affected by animal sources of the precursor heparin, which have different structural compositions,[14,15] and by the production process which might be different based on production date or/and producer. There has been no systematic investigation of the structural differences or similarities between enoxaparins prepared at different times, by different processes, and from different animal sources. It is important to understand how such structural variation can impact the anticoagulant activity of this important drug product.

The structural complexity of heparin and LMWHs was better understood after the heparin crisis in 2007–2009.[16,17] In this crisis, nearly 200 patients died from the heparin they were administered, the heparin being contaminated with a heparinoid, called oversulfated chondroitin sulfate (OSCS).[18] Moreover, some LMWHs including enoxaparin were also reported to be contaminated with OSCS.[19] After the heparin crisis, many methods including chromatography, capillary electrophoresis (CE), mass spectrometry (MS) and nuclear magnetic resonance (NMR) were developed and applied to elucidate the structure of heparin and LMWHs for manufacturing, quality control and glycomics purposes.[20–26] Disaccharide analysis and oligosaccharide mapping methods relying on various chromatographic and hyphenated techniques are now major approaches for accurately understanding the basic structural domains and the dispersities/compositions of saccharides in heparin and LMWHs.[23,24,27] Moreover, a multiple heart-cut 2D liquid chromatography coupled with mass spectrometry (MHC-2DLC-MS), developed in our lab, currently provides some of the best resolution and fingerprint analysis of enoxaparin.[28]

In this study, 38 lots of enoxaparin (Table 1), prepared in different years, by different providers and from different animal sources, were systematically analyzed. Ultra-high-performance size-exclusion chromatography (UHPSEC) was used to analyze the oligosaccharide dispersity and size compositions of enoxaparins. Strong anion exchange (SAX) chromatography was used to analyze the structural composition (disaccharide domains) of enoxaparins after exhaustive digestion with a mixture of heparinases. The chromatographic peaks in both oligosaccharide mapping and disaccharide analysis were integrated. The content of each peak in oligosaccharide mapping and disaccharide analysis was evaluated using principal component analysis (PCA). These data provide clues as to whether the structural variations in enoxaparin, observed in oligosaccharide mapping and/or disaccharide analysis, are attributed to the differences of animal sources of its heparin precursor or the enoxaparin production processes used by different manufacturers. The representative samples were fingerprinted with MHC-2DLC-MS, in which the detailed glycan composition of each enoxaparin would be profiled. Finally, the binding capacities of these 38 lots of enoxaparins to AT were determined using surface plasmon resonance (SPR) operating under the competitive inhibition mode and the relationships between the structural variation and production times, brands, animal sources and AT binding affinity are discussed in this

Table 1 Sample information of enoxaparin sodium

Sample name	Brand or provider	Sources	Production time
Enox EP	EP	Porcine intestinal mucosa	
Enox USP	USP	Porcine intestinal mucosa	
Enox P1	Sanofi	Porcine intestinal mucosa	1980s
Enox P2	Sanofi	Porcine intestinal mucosa	1980s
Enox P3	Sanofi	Porcine intestinal mucosa	1980s
Enox P4	Sanofi	Porcine intestinal mucosa	1980s
Enox P5	Sanofi	Porcine intestinal mucosa	1980s
Enox C1	Sanofi	Porcine intestinal mucosa	1990s
Enox C2	Sanofi	Porcine intestinal mucosa	1990s
Enox C3	Sanofi	Porcine intestinal mucosa	1990s
Enox C4	Sanofi	Porcine intestinal mucosa	1990s
Enox C5	Sanofi	Porcine intestinal mucosa	1990s
Enox E1	Sanofi	Porcine intestinal mucosa	2010–2012
Enox E2	Sanofi	Porcine intestinal mucosa	2010–2012
Enox E3	Sanofi	Porcine intestinal mucosa	2010–2012
Enox E4	Sanofi	Porcine intestinal mucosa	2010–2012
Enox E5	Sanofi	Porcine intestinal mucosa	2010–2012
Enox E6	Sanofi	Porcine intestinal mucosa	2010–2012
Enox E7	Sanofi	Porcine intestinal mucosa	2010–2012
Enox E8	Sanofi	Porcine intestinal mucosa	2010–2012
Enox E9	Sanofi	Porcine intestinal mucosa	2010–2012
Enox E10	Sanofi	Porcine intestinal mucosa	2010–2012
Enox E11	Sanofi	Porcine intestinal mucosa	2010–2012
Enox N1	Sanofi	Porcine intestinal mucosa	2015
Enox N2	Sanofi	Porcine intestinal mucosa	2015
Enox N3	Sanofi	Porcine intestinal mucosa	2015
Enox N4	Sanofi	Porcine intestinal mucosa	2015
Enox N5	Sanofi	Porcine intestinal mucosa	2015
Enox R1	Ronnsi	Porcine intestinal mucosa	2016
Enox R2	Ronnsi	Porcine intestinal mucosa	2016
Enox R3	Ronnsi	Porcine intestinal mucosa	2016
Enox R4	Ronnsi	Ovine intestinal mucosa	2016
Enox R5	Ronnsi	Ovine intestinal mucosa	2017
Enox R6	Ronnsi	Bovine intestine heparin	2015
Enox R7	Ronnsi	Bovine lung heparin	2015
Enox JF1	Dr Fareed	Ovine intestinal mucosa	2016
Enox JF2	Dr Fareed	Bovine intestine heparin	2016
Enox JF3	Dr Fareed	Porcine intestinal mucosa	2016

work. Multiple offline and online chromatographic analyses are the foundation of these studies.

Results and discussion

Oligosaccharide mapping

The MW and oligosaccharide distribution are critical for characterizing the degree of degradation of heparin required to produce enoxaparin. These are also important factors in controlling the efficacy and safety (bleeding or heparin-induced thrombocytopenia, HIT) of an enoxaparin. SEC is the best way to determine oligosaccharide size distribution. The glycans with different sizes in enoxaparin were well separated using the SEC method in this study (Fig. 2). According to our previous publication,[28] the degree of polymerization (dp) of oligosaccharides was assigned from dp2 to dp28 in Fig. 2A. This method resolves smaller oligosaccharides better than bigger ones. Two peaks, observed for each of the dp3, dp4 and dp6 components, were integrated separately. Broad peaks, corresponding to each oligosaccharide from dp8 to >dp28, were individually integrated. The integrated chromatogram for the USP enoxaparin standard sample is shown in Fig. 2A. The representative enoxaparin chromatograms including different batches, producers and animal sources are also shown in Fig. 2. The chromatographic profiles of enoxaparin USP and EP standards were identical (Fig. 2A and B). The chromatographic profiles of N and E batches, produced recently by Sanofi, are also the same as that of enoxaparin standards (ESI Fig. S-1 and S-2†). A representative chromatogram is shown in Fig. 2C. Batch C was produced two decades ago. Their SEC chromatographic profiles are also the same as that of the standards (Fig. 2D and ESI Fig. S-3†). The chromatographic profiles of batch P, which were produced three decades ago, are different from that of enoxaparin standards (Fig. 2E and ESI Fig. S-4†) as more dp2 and dp3 were observed. Additionally, the ratio of two dp4 and two dp6 peaks is significantly different from those of the standards. The shoulder peak observed at 39.1 min, which corresponds to dp5 according to our previous work,[28] is more significant than the shoulder peaks of other enoxaparins. Their chromatographic profiles are more like those of R6 (Fig. 2F) and JF2 (ESI Fig. S-5†), provided by Ronnsi, Ltd and Dr Fareed, respectively, which were produced from bovine intestinal mucosal heparin. The chromatographic profiles of porcine-sourced R batches are similar (ESI Fig. S-6†). The chromatographic profiles of ovine-sourced enoxaparins (R4, R5, JF1) and bovine lung-sourced enoxaparin (R7) are similar (ESI Fig. S-7†). The SEC profiles of representative ovine-sourced and bovine lung-sourced samples (R4 and R7) are shown in Fig. 2G and H. The ratios of the two dp6 oligosaccharides were slightly different from that of porcine-sourced enoxaparin standards.

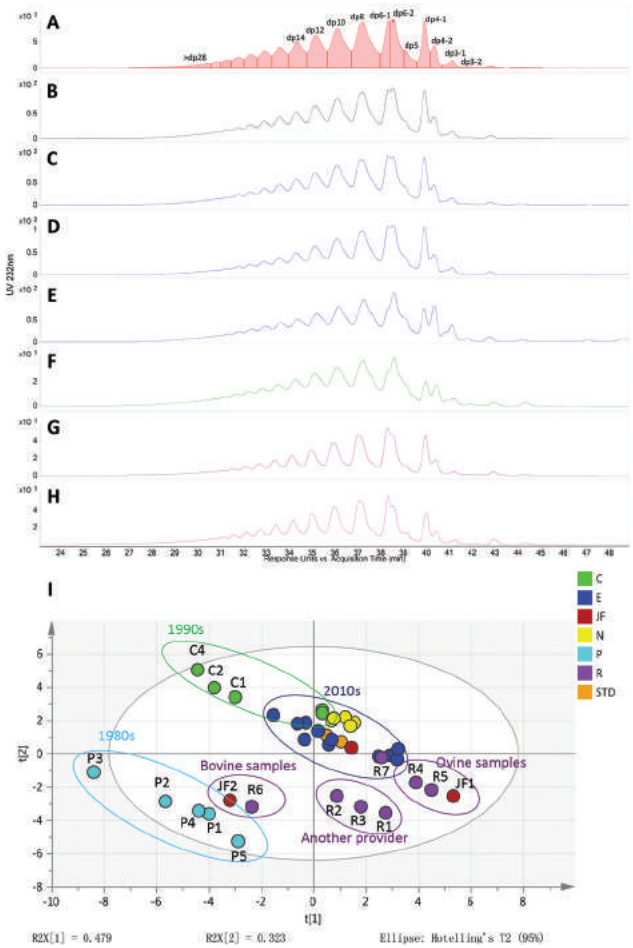

Fig. 2 Size exclusion chromatograms of the representative enoxaparins and PCA analysis. A, Integrated chromatogram of USP enoxaparin; B–H, chromatograms of EP, E1, C1, P1, R6 (bovine intestinal sample), R4 (ovine intestinal sample) and R7 (bovine lung sample); I, PCA of 38 enoxaparin samples based on the SEC results.

The stability of this method, the foundation of our PCA analysis, had been demonstrated in an earlier report.[28] The PCA was plotted in Fig. 2I based on the peak areas integrated in each sample coming from Fig. 2A. Batches E, N and C3/5 are grouped with EP and USP standards. The PCA data points for C1, 2 and 4 were slightly separated from the major group of data. The P, R6 and JF2 batches were widely separated. Samples R1–3 were grouped and slightly separated from that big group. The PCA data points for R4, 5 and JF1 were close to each other as a group. Based on the grouping and dispersion of these PCA data points, the size distributions of enoxaparin correlate to the production date and to some degree the process used by different companies.

Disaccharide compositional analysis

Enoxaparin, like heparin, is mainly composed of repeating disaccharide units. The degree and position of sulfation in these disaccharide units are different and contribute to the complexity of enoxaparin's structure. Thus, disaccharide compositional analysis is critical for the structural elucidation of enoxaparin. All the disaccharide units, as well as some minor structural domains within enoxaparin, were detected in this study and are presented in Table 2. Chromatograms illustrating the disaccharide composition of representative enoxaparin samples are shown in Fig. 3 and the peak assignments are presented in

Table 2 Major and minor structure compositional domains of enoxaparin

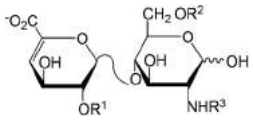

Major domains	R1	R2	R3
ΔIS	SO_3H	SO_3H	SO_3H
ΔIIS	H	SO_3H	SO_3H
ΔIIIS	SO_3H	H	SO_3H
ΔIVS	H	H	SO_3H
ΔIA	SO_3H	SO_3H	H
ΔIIA	H	SO_3H	H
ΔIIIA	SO_3H	H	H
ΔIVA	H	H	H

Minor domains		Structural information
a	$Glyser_{ox1}$	ΔUA-Gal-Gal-Xyl-CH_2-COOH
b	$ΔIIS_{gal}$	ΔGalA-GlcNS6S
c	1,6 anhydro ΔIS	ΔUA2S-GlcNS-1,6-anhydro
d	$ΔIIA\text{-}IIS_{glu}$	ΔUA-GlcNAc6S-GlcA-GlcNS3S6S
e	$ΔIS\text{-}IIS_{glu}$	ΔUA2S-GlcNS6S-GlcA-GlcNS3S6S
f	1,6 anhydro $ΔIS\text{-}IS_{epi}$	ΔUA2S-GlcNS6S-IdoA2S-ManNS-1,6-anhydro

Fig. 3A. Trisulfated disaccharide (ΔIS) is the major component in all samples. In addition to the eight disaccharides, common to both heparin and enoxaparin, six small peaks, labeled a–e, were also observed in the enoxaparin chromatogram at 18.0, 25.8, 31.0, 37.1, 38.1 and 40.9 min, respectively. Peak a, a signature of the production process, is derived from the linkage domain between heparin and its core protein. Peaks b, d and e correspond to enzyme-resistant domains. Peaks c and f come from specific terminal domains in enoxaparin that contain a 1–6 anhydroglucosamine. The assignments of peaks a–e were previously reported.[32–34] Chromatograms of the disaccharide analysis of representative enoxaparin samples are shown in Fig. 3B–G and detailed structural information of these disaccharide units and domains are provided in Table 2.

The disaccharide compositional analysis results of 38 enoxaparins are presented in ESI Table S-1.† The peak areas are plotted in the PCA presented in Fig. 3I. EP, USP standards and N, E, C batches all clustered into a grouping. All these enoxaparins were produced from porcine intestinal mucosal heparins. Most of the P samples were in a cluster slightly separated from the remaining samples in this big grouping. While most enoxaparins in that big grouping showed little compositional differences, the content of ΔIIIS in P1, P2, P4 and P5 is slightly higher than that in other porcine intestinal mucosal-derived enoxaparin samples and their 1,6 dehydrated ΔIS (peak c) contents were ~2.5% higher than that observed in other samples in this grouping (~1.8%). JF2 and R6, both produced from bovine intestinal heparins, grouped together. These bovine intestinal heparin-derived enoxaparins showed they have slightly higher ΔIVA (~4% *vs.* ~3%), significantly higher ΔIIIS (~16% *vs.* ~6%) and relatively lower ΔIS content (~56% *vs.* 60%) compared to porcine intestinal heparin-derived enoxaparins. JF1, R4 and R5, produced from ovine intestinal mucosal heparins, were also grouped together. They showed significantly higher ΔIS content than porcine-sourced enoxaparins (~71% *vs.* ~60%). R7, produced from bovine lung heparin, has the highest ΔIS content (~76%). P3 was separated from all other samples, having lower ΔIVA, ΔIIA, ΔIIIA, ΔIIS, and ΔIA content, but significantly higher ΔIIIS content (~13% *vs.* ~6%). It should be a combination of porcine and bovine-sourced product. Based on the results of disaccharide compositional analysis, an enoxaparin is most related to the source of its precursor heparin.

Fingerprinting analysis of enoxaparins with MHC-2DLC-MS[28]

Enoxaparins were analyzed with MHC-2DLC-MS to compare their differences. The top of each peak corresponding to dp3, dp4, dp5 and dp6 of enoxaparin observed in the first-dimensional chromatography (1D, SEC) was automatically cut and injected to the second-dimensional chromatography (2D, IPRP) with an MHC system. MS was then used as a detector that also provides structural information. Extracted compound chromatography (ECC) was used in the processing of all the MS data. Each peak in the ECC includes all MS signals corresponding to one oligosaccharide, such as ions with different charge states, different PTA adducts, and fragments associated with in-source sulfate group loss. All peaks were assigned using GlycoResoft 2.0 software.[35] The assignment of structure is based on the known structural properties of enoxaparin. Each oligosaccharide in enoxaparin is described using six numbers, presented in square brackets, corresponding to the number of unsaturated uronic acid residues (ΔUA, 4-deoxy-α-L-*threo*-hex-4-enopyranosyluronic acid), saturated uronic acid residues (IdoA or GlcA), glucosamine residues (GlcN), acetyl groups (Ac), sulfo groups (S) and 1,6 anhydroglucosamine, respectively.[28,35]

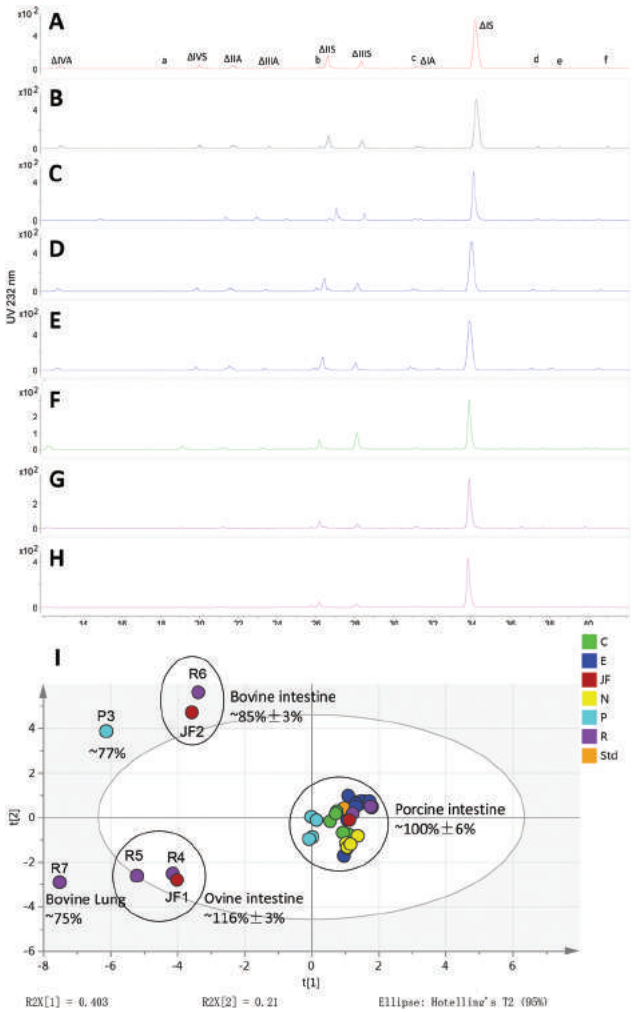

Fig. 3 Strong anion exchange chromatograms of disaccharides derived from the representative enoxaparins and PCA analysis. A–H, Chromatograms of USP, EP, E1, C1, P1, R6 (bovine intestinal sample), R4 (ovine intestinal sample) and R7 (bovine lung sample); I, PCA of 38 enoxaparin samples based on the SAX disaccharide analysis results.

A representative profile of USP enoxaparin for first-dimensional chromatography (SEC) is presented in Fig. 4A. The peaks corresponding to dp5 and two dp6 in SEC were cut and injected to second-dimensional chromatography. The ECC profiles corresponding to dp6-1 of some representative enoxaparin samples, including USP enoxaparin, E1, P1, P3, R4, R6 and R7, are shown in Fig. 4B. The 2D chromatographic profiles of dp6-1 for USP, E1, P1, R6 and R4 samples were the same. The two dominant peaks observed at 6.5 and 6.6 min were assigned as [1;2;3;0;9;0]/[0;3;2;0;9;1]. These two hexasaccharides contain an unsaturated uronic acid, two saturated uronic acid, three glucosamine, and nine sulfo groups or three saturated uronic acid, two glucosamine, one 1,6 anhydroglucosamine and nine sulfo groups. The two small peaks, observed at about 7 min, contain nine sulfo groups, but no unsaturated or 1,6 anhydroglucosamine on either glycan terminus ([0;3;3;0;9;0]). The glycans corresponding to these four peaks are composed of the major tri-sulfated disaccharide domain (ΔIS) in heparin. Four peaks were observed from 5.6 to 6.0 min in ECC. Based on their assignments ([1;2;3;0;8;0]/[0;3;2;0;8;1]), these four peaks in ECC have one sulfo group less than the oligosaccharides observed in the dominant peaks at 6.5 and 6.6 min. These could be unsaturated oligosaccharides with unsaturated uronic acid at the non-reducing end or anhydro oligosaccharides with the 1,6 anhydroglucosamine unit at the reducing end. In addition, lower sulfation generally results in more sequencing possibilities and more isomers are observed. A small peak, observed at 6.2 min, also corresponds to a saccharide with eight sulfo groups ([1;2;2;0;8;1]), but with both unsaturated uronic acid and 1,6 anhydro glucosamine residues. No significant differences were observed in the dp6-1 ECC of P3 and R7, but the contents of less sulfated oligosaccharides observed at 5.6 to 6.2 were lower than those observed in USP, E1, P1 and R4 enoxaparins.

The ECC profiles corresponding to dp6-2 of these representative samples, including USP enoxaparin, E1, P1, P3, R4, R6 and R7, are shown in Fig. 4C. The ECC profiles of USP, E1 and P1 are identical with eight small peaks observed from 4.4 to 5.1 min. These corresponded to hexasaccharides having 7 sulfo groups. The first four were assigned as [1;2;3;0;7;0]/[0;3;2;0;7;1], and the middle two had one acetyl group and were assigned as [1;2;3;1;7;0]/[0;3;2;1;7;1]. Five major peaks were observed from 5.7 to 6.3 min and all of these corresponded to hexasaccharides having 8 sulfo groups. The first three peaks were assigned as [1;2;3;0;8;0]/[0;3;2;0;8;1] and the last two peaks were assigned as [1;2;2;0;8;1]. Both unsaturated uronic acid and 1,6 anhydroglucosamine residues were present in these two hexasaccharides. Four small peaks were observed at 6.5 to 7.1 min and all corresponded to hexasaccharides having 9 sulfo groups. The first two were assigned as [1;2;3;0;9;0]/[0;3;2;0;9;1] and the last two were assigned as [0;3;3;0;9;0], neither of which contained unsaturated uronic acid and 1,6 anhydroglucosamine. Compared to the USP sample, a lower content of hexasaccharides having 7 sulfo groups was observed in P3. A higher content of hexasaccharides having 7 sulfo groups was observed in R6 (derived from bovine intestinal mucosal heparin). Both of these had a lower content of hexasaccharides having 9 sulfo groups. These rare hexasaccharides having 7 sulfo groups were observed in R7 (bovine lung sample). However, a lower content of oligosaccharides having 7 sulfo groups and a higher content of oligosaccharides having 9 sulfo groups were observed in R4 (derived from ovine intestinal heparin).

The ECC profiles corresponding to dp5 of these representative samples, including USP enoxaparin, E1, P1, P3, R4, R6 and R7, are shown in Fig. 4D. In the ECC of these samples, the major peaks correspond to pentasaccharides, but most of the minor peaks are hexasaccharides having a low number of sulfo groups. The ECC profiles of USP, E1 and P1 were identical. A small peak, observed at 2.6 min, was assigned as [1;2;3;1;5;0]/[0;3;2;1;5;1] and the peaks at 3.5 to 4.2 min corresponded to hexasaccharides having 6 sulfo groups. The first three were assigned as [1;2;3;0;6;0]/[0;3;2;0;6;1] and the last three were

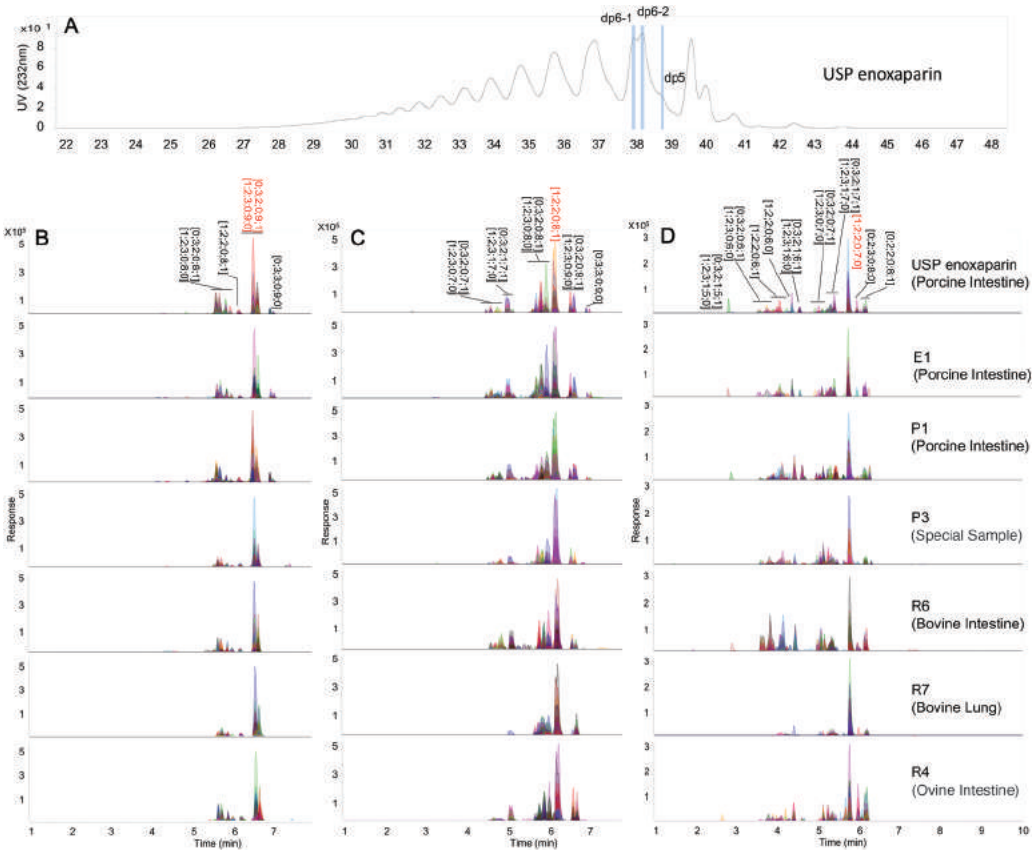

Fig. 4 ECC of dp6-1, 6-2 and 5 of enoxaparins based on MHC-2DLC-MS results. A, ^{1}D chromatogram of USP enoxaparin; B, ECCs of dp6-1 of USP, E1, P1, P3, R4, R6 and R7; C, ECCs of dp6-2 of USP, E1, P1, P3, R4, R6 and R7; D, ECCs of dp5 of USP, E1, P1, P3, R4, R6 and R7.

assigned as [1;2;2;0;6;1]. The peak observed at 4.3 min corresponded to a pentasaccharide having 6 sulfo groups assigned as [1;2;2;0;6;0]. The peak observed at 4.5 min corresponded to a hexasaccharide with 6 sulfo and one acetyl groups assigned as [1;2;3;1;6;0]/[0;3;2;1;6;1]. The six small peaks observed from 5.0 to 5.6 min corresponded to seven sulfated hexasaccharides with 7 sulfo groups, in which the last two compounds were mono-acetylated. The dominant peak observed at 5.8 min corresponded to a pentasaccharide having 7 sulfo groups and was assigned as [1;2;2;0;7;0]. Its content corresponded to over 80% of the total peak area. The small peaks observed from 6.0 to 6.2 min corresponded to pentasaccharides with 8 sulfo groups and were assigned as [0;2;3;0;8;0] and [0;2;2;0;8;1], respectively. Few acetylated oligosaccharides were observed in the P3 enoxaparin. This sample also had a lower content of pentasaccharides with 8 sulfo groups. The content of oligosaccharides having reduced sulfation was significantly higher in R6 (derived from bovine intestinal heparin) than that observed in the USP sample, but acetylated oligosaccharides were rarely observed. The content of the dominant pentasaccharide with 7 sulfo groups corresponds to more than 90% in R7 (derived from bovine lung heparin), while the other oligosaccharide components are much lower than observed in the other samples. A higher content of highly sulfated oligosaccharides, and greater variety of undersulfated hexasaccharides were observed in the ECC of R4 (derived from ovine intestinal heparin).

The peaks corresponding to the two dp4 and dp3 components observed in SEC were cut and injected to the second-dimensional chromatography using the MHC system (see ESI†). The ECC profiles, corresponding to dp4-1, are representative of USP enoxaparin, E1, P1, P3, R4, R6 and R7, showing no significant differences (ESI Fig. S-8B†) and two major peaks corresponding to tetrasaccharides with 6 sulfo groups, assigned as [1;1;2;0;6;0]/[0;2;1;0;6;1] and [0;2;2;0;6;0], respectively.

The ECC profiles corresponding to dp4-2 for these same samples are shown in ESI Fig. S-8C.† The peaks observed from 2.5 to 2.9 min correspond to tetrasaccharides with 5 sulfo groups, all assigned as [1;1;2;0;5;0] or [0;2;1;0;5;1]. The major peaks observed at 3.1 min were also tetrasaccharides with 5 sulfo groups and assigned as [1;1;1;0;5;1]. No significant differences in the profiles of USP enoxaparin, E1, P1, P3, R4, R6 and R7 were observed.

The ECC profiles corresponding to dp3 of USP enoxaparin, E1, P1, P3, R4, R6 and R7 are shown in ESI Fig. S-8D.† The ECC profiles of USP, E1 and P1 are identical. The peaks from 1.9 to 2.0 min are tetrasaccharides with 4 sulfo groups, assigned as [1;1;2;0;4;0]/[0;2;1;0;4;1]. The dominant peak observed at 2.1 min corresponds to the trisaccharide

[1;1;1;0;4;0]. More tetrasaccharides with 4 sulfo groups were observed in P3 and a higher content of tetrasaccharides with 4 sulfo groups was observed in R6 (derived from bovine intestinal heparin). A lower content of tetrasaccharides with 4 sulfo groups was observed in R7 (derived from bovine lung heparin) and R4 (derived from ovine intestinal heparin).

The ECC profiles of different size oligosaccharides in enoxaparins from porcine intestine are similar. Compared to the results of enoxaparins derived from porcine intestine, enoxaparins derived from bovine intestine have a higher content of undersulfated glycans in oligosaccharides of each size. Bovine lung-derived enoxaparin had a much lower content and much lower variety of such undersulfated glycans in oligosaccharides of each size. Ovine intestine-derived enoxaparin had a greater content of highly sulfated glycans and a reduced content of undersulfated glycans but a higher variety of these undersulfated glycans.

AT binding affinity evaluation with surface plasmon resonance (SPR)

The AT binding affinity of the various enoxaparin samples were determined using SPR in the competitive inhibition mode. The data obtained is shown in the ESI.† In the control, AT interacts with immobilized heparin on the chip, without inhibition, and shows a high response unit (RU) binding (Fig. 5A, black curve). R4, R5 and JF1 added into the solution phase blocks the binding of AT to the immobilized heparin showing greatly reduced RU in Fig. 5A (red curves), suggesting that they have the highest binding affinity for AT. Enoxaparin USP and EP and the batches N, E, C, P1, P2, P4, P5, R1, R2 and R3, derived from porcine intestinal heparin, with intermediate RU values (Fig. 5A, five representative blue curves) displayed intermediate binding affinity to AT. Two enoxaparins (R6 and JF2) derived from bovine intestinal heparin showed higher RU (Fig. 5A, cyan curves) and, thus, slightly lower affinity for AT than the enoxaparins derived from porcine intestinal heparin. R7 derived from bovine lung heparin showed the highest RU of all the enoxaparin samples (Fig. 5A, pink curves) and the lowest AT binding affinity. The average ΔRU value of porcine-sourced enoxaparins was normalized to 100%; the average ΔRU values of enoxaparins from ovine intestine, bovine intestine and bovine lung were ~116%, ~85% and ~75%, respectively (Fig. 5B and ESI Table S-2†). P3, the special sample, also showed relatively low activity. The RU values determined in competitive SPR are not only proportional to AT binding affinity but based on previous reports also correlate to the anticoagulant, anti-factor Xa, activity of enoxaparin samples.

Experimental section

Materials

Enoxaparin standards were obtained from the European Pharmacopeia (EP, Strasbourg, France) and the United States Pharmacopeia (USP, Rockville, MD). Eight unsaturated heparin disaccharide standards were purchased from Iduron (London, UK). Heparin lyase I, II and III from recombinant *Flavobacterium heparinum* were purchased from Aglyco (Beijing, China). Antithrombin III (AT) was obtained from HYPHEN BioMed (Neuville-sur-Oise, France). Streptavidin (SA) chip and HBS-EP running buffer containing 0.01 M HEPES, 0.15 M NaCl, 3 mM EDTA, and 0.005% surfactant P20, (pH 7.4) were purchased from GE Healthcare (Uppsala, Sweden). Heparin USP standard and biotin were obtained from Celsus Laboratories (Ohio, USA) and Thermo Fisher Scientific (Massachusetts, USA), respectively.

Waters ACQUITY UPLC® BEH 200 Å SEC (1.7 μm, 4.6 × 300 mm), Waters ACQUITY UPLC® BEH 125 Å SEC (1.7 μm, 4.6 × 300 mm) and Waters ACQUITY UPLC peptide BEH C18, 300 Å (1.7 μm, 2.1 × 100 mm) were obtained from Waters Corporation (Milford, MA, USA). Welch Ultimate XB-SAX (4.6 mm × 250 mm, 3 μm) obtained from Welch Materials, Inc. (Austin, TX). Methanol (HPLC grade) and ammonium acetate (HPLC grade) were purchased from Fisher Scientific

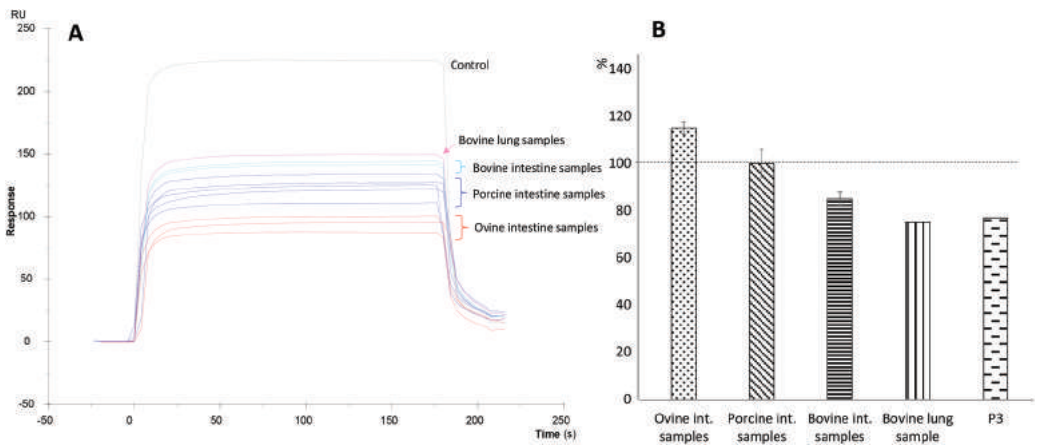

Fig. 5 AT binding affinity results from SPR. A, SPR curves of the representative samples; B, normalized AT binding affinity of enoxaparins from different animal sources based on ΔRU from SPR.

(Springfield, NJ). Sodium phosphate monobasic (HPLC grade) and sodium perchlorate (HPLC grade) were obtained from Millipore Sigma (Burlington, MA). Other chemical reagents were all LC-MS grade. All solutions were prepared in ultrapure water (≥18 MΩ) purified by a Milli-Q water purifier.

Sample information

Current enoxaparin standards were obtained from the EP and USP. Enoxaparin batches (E, C and P series) produced at different production times by Sanofi were kindly provided by Dr Fareed of Loyola University Medical Center, Maywood, IL. Enoxaparin batches (N series) were obtained from the Chinese market. Enoxaparin batches (R series) were kindly provided by Ronnsi. Co. Ltd (Suzhou, China), in which R1–R3 were prepared from porcine intestinal mucosal heparin, R4/R5 were prepared from ovine intestinal mucosal heparin, R6 was prepared from bovine intestinal mucosal heparin, and R7 was prepared from bovine lung heparin. Enoxaparin batches JF1–3 were kindly provided by Dr Fareed from Loyola University Medical Center, Maywood, that were prepared from ovine, bovine and porcine intestinal mucosal heparins, respectively. Detailed sample information is provided in Table 1.

Oligosaccharide mapping with size exclusion chromatography (SEC)

The experiments were performed on an Agilent 1290 UHPLC system with a 1290 infinity diode array detector (DAD). Two SEC columns, 200 Å and 125 Å (both 1.7 μm and 4.6 × 300 mm), were used in tandem to acquire the maximum degree of separation by the size of enoxaparin oligosaccharides. The flow rate was set at 150 μL min^{-1} with an isocratic mobile phase of 50 mM ammonium acetate (H_2O/MeOH, 90 : 10). The sample (10 μg μL^{-1}, 3 μL) was eluted at room temperature and detected at 232 nm. Each peak corresponding to a different degree of polymerization (dp) was integrated. Their percentages were used for further principal component analysis (PCA).

Disaccharide analysis with strong anion exchange chromatography (SAX)

Disaccharides of enoxaparin were prepared by exhaustive digestion using a mixture of heparin lyases I, II, and III (each lyase 0.1 IU per 1.0 mg sample) in buffer (50 mM ammonium acetate containing 2 mM calcium chloride adjusted to pH 7.0) at 37 °C overnight. Enzymatic digestion was terminated by boiling the samples for 10 min and removing the denatured enzymes with centrifugation at 10 000 rpm for 10 min.

The disaccharide analysis was performed on an Agilent 1260 system using a Welch Ultimate XB-SAX column (4.6 mm × 250 mm, 3 μm) at 40 °C and detected at 232 nm. Mobile phase A was 2 mM sodium dihydrogen phosphate aqueous solution. Mobile phase B is 2 mM sodium dihydrogen phosphate and 1.2 M sodium perchlorate aqueous solution. Their pH values were adjusted to 3.0 with phosphoric acid before use. The flow rate was set at 0.6 mL min^{-1}. The mobile phase B increased from 3% to 35% during the first 20 min, then increased to 100% in the next 30 min for the analysis.

Principal component analysis (PCA)

Principal component analysis (PCA), one of the most important multivariate analyses, is a mathematical algorithm that reduces the dimensionality of the data while retaining most of the variation within a data set.[29,30] Using a few components, each sample can be represented by a few numbers rather than by values for thousands of variables. Samples can then be plotted, making it possible to visually assess similarities and differences between samples and determine whether samples can be grouped.

The precision of the analytical methods is critical for PCA as the real structural variations of enoxaparins can be successfully distinguished and grouped only if the analytical methods used have small systematic errors. In this work, the peak ratios in oligosaccharide mapping with HPSEC-UV and disaccharide analysis with SAX-UV were applied for PCA. The stabilities of these two methods are good.[28] The proper PCA results rely on the stabilities of these two methods. The software SMICA 13.0 provided by Umetrics (Umeå, Sweden) was used for data processing.

Fingerprinting analysis of enoxaparins with MHC-2DLC-MS[28]

The experiments were performed on an Agilent two-dimensional UHPLC system with a Q/TOF MS system (1290/1290, dual pump/dual pump, 6540, AGI). Two size-exclusion columns (Waters, SEC BEH 125 Å and 200 Å, 1.7 μm, 4.6 × 300 mm) were used in the first-dimensional chromatography (1D) at 150 μL min^{-1} with an isocratic mobile phase of 50 mM ammonium acetate (water/MeOH, 90 : 10). The sample solution (20 mg mL^{-1}, 3 μL) was eluted at 30 °C and detected at 232 nm. A C18 column (Waters ACQUITY UPLC peptide BEH C18, 300 Å, 1.7 μm, 2.1 × 100 mm) was applied in the second-dimensional chromatography (2D) at 40 °C with a multi-step gradient, in which the mobile phase A was 0.2% pentylamine (PTA) and 0.15% hexafluoroisopropanol (HFIP) aqueous solution; mobile phase B is 0.2% PTA and 0.15% HFIP in 75% acetonitrile. The flow rate was set at 400 μL min^{-1}.

The two dimensions of the system were interconnected by a new multiple heart-cutting (MHC) interface. This interface incorporates a 2-pos/4-port valve to which a selector valve was coupled. The valve is electronically controlled by external drives. The selector valve bears two clusters of six sampling loops (10 μL each). This makes a parking deck with 12 loop positions. The deck permits sampling/parking of targeted aliquots of the effluent from the 1D column. The parked aliquots were automatically injected orderly to second column for further separation. The 2D column was equilibrated for 20 min with 5% mobile phase B between two peaked aliquot injections.

Surface plasmon resonance (SPR)

Binding between enoxaparin and AT was measured using SPR utilizing a competitive inhibition strategy with a Biacore 3000

system (GE, Uppsala, Sweden). SPR is a rapid and real-time method to evaluate the AT binding affinity of enoxaparins.[31] The unfractionated heparin standard was biotinylated and immobilized on three channels of the SA chip. The intensity should have a no less than 200 resonance unit (RU) increase to make sure that immobilization was successful. One flow cell, containing immobilized biotin, served as a control. Each enoxaparin prepared at the concentration of 20 μg mL^{-1} was premixed with AT solution (323 nM L^{-1}) in running buffer (HBS-EP) and incubated at 37 °C for 8 min prior to injection. The running buffer was eluted at a flow rate of 30 μL min^{-1} at 25 °C. The response was monitored in real time. Before every analysis, 30 μL of 2 M NaCl was used to regenerate the chip surface and 30 μL of running buffer (HBS-EP) was used to equilibrate the chip.

Conclusion

In this study, the size distribution, structural composition and AT binding affinities of 38 enoxaparins were systematically analyzed including batches produced in the 1980s, 1990s and 2010s by the original manufacturer (Sanofi), batches from other providers and batches from other animal-sourced heparin products. The relationships between size distribution/production processes/AT binding affinity and disaccharide composition/animal sources/AT binding affinity were investigated, discussed and confirmed with experimental evidence. Fingerprinting analysis provided deeper insight into the size and structural compositions of these enoxaparins and provided comprehensive information to more clearly understand the relationship between structure and AT binding-based anticoagulant activity about enoxaparins.

The slight differences in the size distribution of enoxaparins was attributed to the process used in their production, and were likely different in batches made on different dates and by different producers. Furthermore, the AT binding affinity does not correlate with the size distribution of these enoxaparins.

Both of the structural compositions and AT binding affinities of these enoxaparins are related to their animal sources. The trisulfated disaccharide, corresponding to the major domain of heparins and enoxaparins, was ~71%, ~60% and ~55% in ovine, porcine and bovine intestinal-derived samples, respectively. Interestingly, their AT binding affinities followed the same order; however, the bovine lung sample with the most trisulfated disaccharide (~75%) showed the lowest AT binding affinity, thus preventing a generalizable rule relating the disaccharide composition of an enoxaparin to its AT binding affinities. This is not surprising as AT binding affinity is known to be directly related to the AT pentasaccharide binding site, which itself is actually deficient in trisulfated disaccharide units.[10,11]

More structural and compositional information was provided by fingerprint analysis. The results suggest that both the variety and sulfation levels of the glycans comprising an enoxaparin contribute to its AT binding affinity. This is again consistent with the known structural complexity and known structural variability of the AT pentasaccharide binding site responsible for the anticoagulant activity of enoxaparin.[36]

P3 appears to be derived from a mixture of porcine intestinal, bovine intestinal and bovine lung heparins, as the contents and/or compositions of glycans shown in its ECCs were always in the middle of those of porcine and bovine samples. The disaccharide composition of P3 also implies the combination of the porcine sample with bovine samples. The SEC profiles of P batches and bovine lung samples (R6 and JF2) are similar, but their ECC profiles are different, more strongly supporting the fact that the glycan size distribution in enoxaparin is more related to the production process but not to animal sources.

This study reflects the real situation of enoxaparin. An animal source was not required and quality control was weak in pharmacopeias before enoxaparin's structure could be elucidated in detail. Nowadays, the quality of enoxaparin should be well defined and controlled with the development of analytical techniques and deeper understanding of the relationships between structure/function, structure/process and structure/animal sources.

Conflicts of interest

There are no conflicts to declare.

Acknowledgements

The authors are grateful to the National Natural Science Foundation of China (81473179 and 81673388), and the funding for the Jiangsu Key Laboratory of Translational Research and Therapy for Neuro-Psycho-Diseases (BM2013003). We also thank Dr Fareed from Loyola University Medical Center, Maywood, and Ronnsi Co., Ltd, for kindly providing LMWH samples.

References

1 R. G. Ingle and A. S. Agarwal, *Carbohydr. Polym.*, 2014, **106**, 148–153.
2 J. I. Weitz, *N. Engl. J. Med.*, 1997, **337**, 688–699.
3 D. Zhao, Q. Sang and H. Cui, *Biomed. Pharmacother.*, 2016, **79**, 194–200.
4 R. J. Linhardt and N. S. Gunay, *Semin. Thromb. Hemostasis*, 1999, **25**, 5–16.
5 H. Liu, Z. Zhang and R. J. Linhardt, *Nat. Prod. Rep.*, 2009, **26**, 313–321.
6 D. Wardrop and D. Keeling, *Br. J. Haematol.*, 2008, **141**, 757–763.
7 B. Mulloy, A. Heath, Z. Shriver, F. Jameison, A. Al Hakim, T. S. Morris and A. Y. Szajek, *Anal. Bioanal. Chem.*, 2014, **406**, 4815–4823.

8 Z. Shriver, I. Capila, G. Venkataraman and R. Sasisekharan, Heparin and Heparan Sulfate: Analyzing Structure and Microheterogeneity, in *Heparin, a Century of Progress*, ed. R. Lever, B. Mulloy and C. P. Page, Springer Berlin Heidelberg, Berlin, Heidelberg, 2012, vol. 207, pp. 159–176.

9 A. Onishi, K. St Ange, J. S. Dordick and R. J. Linhardt, *Front. Biosci., Landmark Ed.*, 2016, **21**, 1372–1392.

10 U. Lindahl, G. Bäckström, L. Thunberg and I. G. Leder, *Proc. Natl. Acad. Sci. U. S. A.*, 1980, **77**, 6551–6555.

11 R. J. Linhardt, *J. Med. Chem.*, 2003, **46**, 2551–2564.

12 Y. Ouyang, Y. Zeng, L. Yi, H. Tang, D. Li, R. J. Linhardt and Z. Zhang, *J. Chromatogr. A*, 2017, **1522**, 56–61.

13 I. Capila and R. J. Linhardt, *Angew. Chem., Int. Ed.*, 2002, **41**, 390–412.

14 X. Liu, K. Stange, J. Fareed, D. Hoppensteadt, W. Jeske, A. Kouta, L. Chi, C. Jin, Y. Jin, Y. Yao and R. J. Linhardt, *Clin. Appl. Thromb./Hemostasis*, 2017, **23**, 542–553.

15 Y. B. Monakhova, B. W. K. Diehl and J. Fareed, *J. Pharm. Biomed. Anal.*, 2018, **149**, 114–119.

16 C. T. Laurencin and L. Nair, *Nat. Biotechnol.*, 2008, **26**(6), 621–623.

17 T. K. Kishimoto, K. Viswanathan, T. Ganguly, S. Elankumaran, S. Smith, K. Pelzer, J. C. Lansing, N. Sriranganathan, G. Zhao, Z. Galcheva-Gargova, A. Al-Hakim, G. S. Bailey, B. Fraser, S. Roy, T. Rogers-Cotrone, L. Buhse, M. Whary, J. Fox, M. Nasr, G. J. Dal Pan, Z. Shriver, R. S. Langer, G. Venkataraman, K. F. Austen, J. Woodcock and R. Sasisekharan, *N. Engl. J. Med.*, 2018, **358**(23), 2457–2467.

18 M. Guerrini, D. Beccati, Z. Shriver, A. Naggi, K. Viswanathan, A. Bisio, I. Capila, J. C. Lansing, S. Guglieri, B. Fraser, A. Al-Hakim, N. S. Gunay, Z. Zhang, L. Robinson, L. Buhse, M. Nasr, J. Woodcock, R. Langer, G. Venkataraman, R. J. Linhardt, B. Casu, G. Torri and R. Sasisekharan, *Nat. Biotechnol.*, 2008, **26**, 669–775.

19 Z. Zhang, M. Weïwer, B. Li, M. M. Kemp, T. H. Daman and R. J. Linhardt, *J. Med. Chem.*, 2008, **51**, 5498–5501.

20 M. Guerrini, Z. Zhang, Z. Shriver, A. Naggi, S. Masuko, R. Langer, B. Casu, R. J. Linhardt, G. Torri and R. Sasisekharan, *Proc. Natl. Acad. Sci. U. S. A.*, 2009, **106**, 16956–16961.

21 Z. Zhang, B. Li, J. Suwan, F. Zhang, Z. Wang, H. Liu, B. Mulloy and R. J. Linhardt, *J. Pharm. Sci.*, 2009, **98**, 4017–4026.

22 X. Zhang, V. Pagadala, H. M. Jester, A. M. Lim, T. Q. Pham, A. M. P. Goulas, J. Liu and R. J. Linhardt, *Chem. Sci.*, 2017, **8**, 7883–8466.

23 Q. Q. Zhang, X. Chen, Z. J. Zhu, X. Q. Zhan, Y. F. Wu, L. K. Song and J. W. Kang, *Anal. Chem.*, 2013, **85**(5), 1819–1827.

24 L. Li, F. Zhang, J. Zaia and R. J. Linhardt, *Anal. Chem.*, 2012, **84**(20), 8822–8829.

25 G. Li, J. Steppich, Z. Wang, Y. Sun, C. Xue, R. J. Linhardt and L. Li, *Anal. Chem.*, 2014, **86**(13), 6626–6632.

26 X. Liu, K. St Ange, X. Wang, L. Lin, F. Zhang, L. Chi and R. J. Linhardt, *Anal. Chim. Acta*, 2017, **961**, 91–99.

27 X. Sun, A. Sheng, X. Liu, F. Shi, L. Jin, S. Xie, F. Zhang, R. J. Linhardt and L. Chi, *Anal. Chem.*, 2016, **88**, 7738–7744.

28 Y. Ouyang, Y. Zeng, Y. Rong, Y. Song, L. Shi, B. Chen, X. Yang, N. Xu, R. J. Linhardt and Z. Zhang, *Anal. Chem.*, 2015, **87**, 8957–8963.

29 I. T. Jolliffe and J. Cadima, *Philos. Trans. R. Soc., A*, 2016, **374**, 1–16.

30 J. Lever, M. Krzywinski and N. Altman, *Nat. Methods*, 2017, **14**, 641–642.

31 J. Zhao, X. Liu, A. Malhotra, Q. Li, F. Zhang and R. J. Linhardt, *Anal. Biochem.*, 2017, **526**, 39–42.

32 P. Mourier, P. Anger, C. Martinez, F. Herman and C. Viskov, *Anal. Chem. Res.*, 2015, **3**, 46–53.

33 R. Sadowski, R. Gadzała-Kopciuch, T. Kowalkowski, P. Widomski, L. Jujeczka and B. Buszewski, *J. AOAC Int.*, 2017, **100**, 1706–1714.

34 <207> Test for 1,6-anhydro derivative for enoxaparin sodium.pdf.

35 E. Maxwell, Y. Tan, Y. Tan, H. Hu, G. Benson, K. Aizikov, S. Conley, G. O. Staples, G. W. Slysz, R. D. Smith and J. Zaia, *PLoS One*, 2012, **7**(9), e45474.

36 Y. Chen, J. Zhao, Y. Yu, X. Liu, L. Lin, F. Zhang and R. J. Linhardt, *J. Pharm. Sci.*, 2018, **107**, 1290–1295.